AFRL-RX-WP-JA-2015-0115

PARTIAL COORDINATION NUMBERS IN BINARY METALLIC GLASSES (POSTPRINT)

Daniel B. Miracle
AFRL/RXCM

Kevin Laws
University of New South Wales

Oleg N. Senkov
UES, Inc.

Garth B. Wilks
UTC, Inc.

APRIL 2014
Interim Report

Distribution Statement A. Approved for public release; distribution unlimited.

See additional restrictions described on inside pages

STINFO COPY

©2011 The Minerals, Metals & Materials Society and ASM International

AIR FORCE RESEARCH LABORATORY
MATERIALS AND MANUFACTURING DIRECTORATE
WRIGHT-PATTERSON AIR FORCE BASE OH 45433-7750
AIR FORCE MATERIEL COMMAND
UNITED STATES AIR FORCE

NOTICE AND SIGNATURE PAGE

Using Government drawings, specifications, or other data included in this document for any purpose other than Government procurement does not in any way obligate the U.S. Government. The fact that the Government formulated or supplied the drawings, specifications, or other data does not license the holder or any other person or corporation; or convey any rights or permission to manufacture, use, or sell any patented invention that may relate to them.

Qualified requestors may obtain copies of this report from the Defense Technical Information Center (DTIC) (http://www.dtic.mil).

AFRL-RX-WP-JA-2015-0115 HAS BEEN REVIEWED AND IS APPROVED FOR PUBLICATION IN ACCORDANCE WITH ASSIGNED DISTRIBUTION STATEMENT.

//Signature//

MICHEAL E. BURBA, Project Engineer
Metals Branch
Structural Materials Division

//Signature//

DANIEL J. EVANS, Chief
Metals Branch
Structural Materials Division

//Signature//

ROBERT T. MARSHALL, Deputy Chief
Structural Materials Division
Materials And Manufacturing Directorate

This report is published in the interest of scientific and technical information exchange and its publication does not constitute the Government's approval or disapproval of its ideas or findings.

REPORT DOCUMENTATION PAGE

Form Approved
OMB No. 0704-0188

The public reporting burden for this collection of information is estimated to average 1 hour per response, including the time for reviewing instructions, searching existing data sources, gathering and maintaining the data needed, and completing and reviewing the collection of information. Send comments regarding this burden estimate or any other aspect of this collection of information, including suggestions for reducing this burden, to Department of Defense, Washington Headquarters Services, Directorate for Information Operations and Reports (0704-0188), 1215 Jefferson Davis Highway, Suite 1204, Arlington, VA 22202-4302. Respondents should be aware that notwithstanding any other provision of law, no person shall be subject to any penalty for failing to comply with a collection of information if it does not display a currently valid OMB control number. **PLEASE DO NOT RETURN YOUR FORM TO THE ABOVE ADDRESS**.

1. REPORT DATE *(DD-MM-YY)*	2. REPORT TYPE	3. DATES COVERED *(From - To)*
April 2014	Interim	19 March 2014 – 31 March 2014

4. TITLE AND SUBTITLE
PARTIAL COORDINATION NUMBERS IN BINARY METALLIC GLASSES (POSTPRINT)

5a. CONTRACT NUMBER
In-house

5b. GRANT NUMBER

5c. PROGRAM ELEMENT NUMBER
62102F

6. AUTHOR(S)
See back

5d. PROJECT NUMBER
4349

5e. TASK NUMBER

5f. WORK UNIT NUMBER
X0W6

7. PERFORMING ORGANIZATION NAME(S) AND ADDRESS(ES)
See back

8. PERFORMING ORGANIZATION REPORT NUMBER

9. SPONSORING/MONITORING AGENCY NAME(S) AND ADDRESS(ES)
Air Force Research Laboratory
Materials and Manufacturing Directorate
Wright-Patterson Air Force Base, OH 45433-7750
Air Force Materiel Command
United States Air Force

10. SPONSORING/MONITORING AGENCY ACRONYM(S)
AFRL/RXCM

11. SPONSORING/MONITORING AGENCY REPORT NUMBER(S)
AFRL-RX-WP-JA-2015-0115

12. DISTRIBUTION/AVAILABILITY STATEMENT
Distribution Statement A. Approved for public release; distribution unlimited.

13. SUPPLEMENTARY NOTES
Journal article published *Metallurgical and Materials Transactions A,* Volume 43A, August 2012, 2649-2661.
©2011 The Minerals, Metals & Materials Society and ASM International. The U.S. Government is joint author of the work and has the right to use, modify, reproduce, release, perform, display or disclose the work. This report contains color. The final publication is available at DOI: 10.1007/s11661-011-1002-7.

14. ABSTRACT
A critical analysis of measured partial coordination numbers for binary metallic glasses as a function of composition shows a large scatter of ±1.5 but clear trends. The current work uses two topological models to predict the influence of relative atomic size and concentration on partial coordination numbers. The equations for partial coordination numbers derived from these two models can reproduce measured data within experimental scatter, suggesting that chemical effects on local structure, although present, may be relatively small. Insights gained from these models show that structural site-filling rules are different for glasses with solute atoms that are smaller than solvent atoms and for glasses where solute atoms are larger than solvent atoms. Specifically, solutes may occupy both β and γ intercluster sites when the solute-to-solvent radius ratio R is less than 1.26, but only β sites can be occupied by solutes when R > 1.26. This distinction gives a simple topological explanation for the observed preference for binary metallic glasses with solutes smaller than solvent atoms. In addition to structure-specific equations, simplified phenomenological equations for partial coordination numbers are given as a convenience.

15. SUBJECT TERMS
bulk metallic glasses, partial coordination numbers

16. SECURITY CLASSIFICATION OF:			17. LIMITATION OF ABSTRACT:	18. NUMBER OF PAGES	19a. NAME OF RESPONSIBLE PERSON (Monitor)
a. REPORT	b. ABSTRACT	c. THIS PAGE			Micheal E. Burba
Unclassified	Unclassified	Unclassified	SAR	17	19b. TELEPHONE NUMBER *(Include Area Code)* (937) 255-9795

REPORT DOCUMENTATION PAGE Cont'd

6. AUTHOR(S)

Daniel B. Miracle - AFRL/RXCM

Kevin Laws - University of New South Wales

Oleg N. Senkov - UES, Inc.

Garth B. Wilks - UTC, Inc.

7. PERFORMING ORGANIZATION NAME(S) AND ADDRESS(ES)

AFRL/RXCM
2941 Hobson Way
Bldg 654, Rm 136
Wright-Patterson AFB, OH 45433

School of Materials Science and Engineering
University of New South Wales
Sydney 2052, Australia

UES Inc.
4401 Dayton-Xenia Rd.
Dayton, OH 45432-1894

UTC, Inc.
1270 North Fairfield Rd.
Dayton, OH 45432-2600

Partial Coordination Numbers in Binary Metallic Glasses

DANIEL B. MIRACLE, KEVIN LAWS, OLEG N. SENKOV, and GARTH B. WILKS

A critical analysis of measured partial coordination numbers for binary metallic glasses as a function of composition shows a large scatter of ±1.5 but clear trends. The current work uses two topological models to predict the influence of relative atomic size and concentration on partial coordination numbers. The equations for partial coordination numbers derived from these two models can reproduce measured data within experimental scatter, suggesting that chemical effects on local structure, although present, may be relatively small. Insights gained from these models show that structural site-filling rules are different for glasses with solute atoms that are smaller than solvent atoms and for glasses where solute atoms are larger than solvent atoms. Specifically, solutes may occupy both β and γ intercluster sites when the solute-to-solvent radius ratio R is less than 1.26, but only β sites can be occupied by solutes when $R > 1.26$. This distinction gives a simple topological explanation for the observed preference for binary metallic glasses with solutes smaller than solvent atoms. In addition to structure-specific equations, simplified phenomenological equations for partial coordination numbers are given as a convenience.

DOI: 10.1007/s11661-011-1002-7
© The Minerals, Metals & Materials Society and ASM International 2011

I. INTRODUCTION

THE number and type of atoms that surround a given central atom is the simplest description of atomic structure in metallic glasses. This first-neighbor constitution dictates the number and type of atomic bonds in the structure and so exerts a dominant influence on stability. The first-neighbor constitution also sets the local atomic packing efficiency,[1,2] which controls many physical and mechanical properties, including the mechanisms of deformation. The first-neighbor constitution is given by partial coordination numbers Z_{ij}, which are the number of j atoms in the first shell of a reference i atom. In binary alloys consisting of solute (α) and solvent atoms (Ω), there are four separate partial coordination numbers: $Z_{\alpha\alpha}$, $Z_{\alpha\Omega}$, $Z_{\Omega\alpha}$, and $Z_{\Omega\Omega}$. Only three of these are independent, because $Z_{\alpha\Omega}$ and $Z_{\Omega\alpha}$ are related

$$f_\alpha Z_{\alpha\Omega} = f_\Omega Z_{\Omega\alpha} \quad [1]$$

where f_i is the atomic fraction of atom i. Although recent structural descriptions focus on solute-centered clusters, a complete structural description requires that equal merit be given to both solute-centered and solvent-centered clusters.

DANIEL B. MIRACLE, Senior Scientist, is with the Air Force Research Laboratory, Materials and Manufacturing Directorate, Wright-Patterson AFB, OH 45433. Contact e-mail: Daniel.miracle@wpafb.af.mil KEVIN LAWS, Senior Research Fellow, is with the ARC Centre of Excellence for Design in Light Metals, School of Materials Science and Engineering, University of New South Wales, Sydney 2052, Australia. OLEG N. SENKOV, Senior Researcher, is with the Air Force Research Laboratory, Materials and Manufacturing Directorate, Wright-Patterson AFB, and is also with UES, Inc., Dayton, OH 45432. GARTH B. WILKS, Scientist, is with the UTC, Inc., Wright-Patterson AFB, OH 45433.

Manuscript submitted April 28, 2011.
Article published online December 7, 2011

Partial coordination numbers can be measured using diffraction techniques (see for example, Reference 3). Three independent measurements are needed to separate the overlapping contributions to the total scattering function from the three independent atom pairs in binary alloys, and six independent experiments are needed to resolve Z_{ij} values in ternary alloys. An integrated approach combining experimental data, reverse Monte Carlo calculations, and atomic simulation to deconvolute overlapping peaks has been developed recently to give Z_{ij} values for ternary metallic glasses.[4] The Z_{ij} values for more complex metallic glasses have been estimated[5] using structural concepts from the efficient cluster packing (ECP) model[6,7] to rationalize the insignificance of some weighting factors. As a result of the difficulties associated with the determination of Z_{ij}, relatively little data are available for binary glasses and almost no data are published for partial coordination numbers in higher order glasses.

Measured partial coordination numbers are compiled in a recent assessment of binary metallic glasses.[8] These data are plotted in Figure 1, along with additional data not included in that assessment.[5,9–11] The data show significant scatter, and a critical analysis shows two areas of concern. First, several datasets do not satisfy the required relation between $Z_{\alpha\Omega}$ and $Z_{\Omega\alpha}$ (Eq. [1]). In most cases, deviations from Eq. [1] are probably within experimental error, but in some cases, the discrepancy can be much larger and is sometimes as large as 3. The second issue is that several total coordination numbers around α and Ω, $Z_{\alpha,\mathrm{tot}}$ and $Z_{\Omega,\mathrm{tot}}$, deviate significantly from the values needed for efficient atomic packing and consistency with measured metallic glass densities. In some glasses, the total coordination number is as low as 5 or 6, once again suggesting that errors in some Z_{ij} values might be as large as 3. The experimental data are

Distribution Statement A. Approved for public release; distribution unlimited.

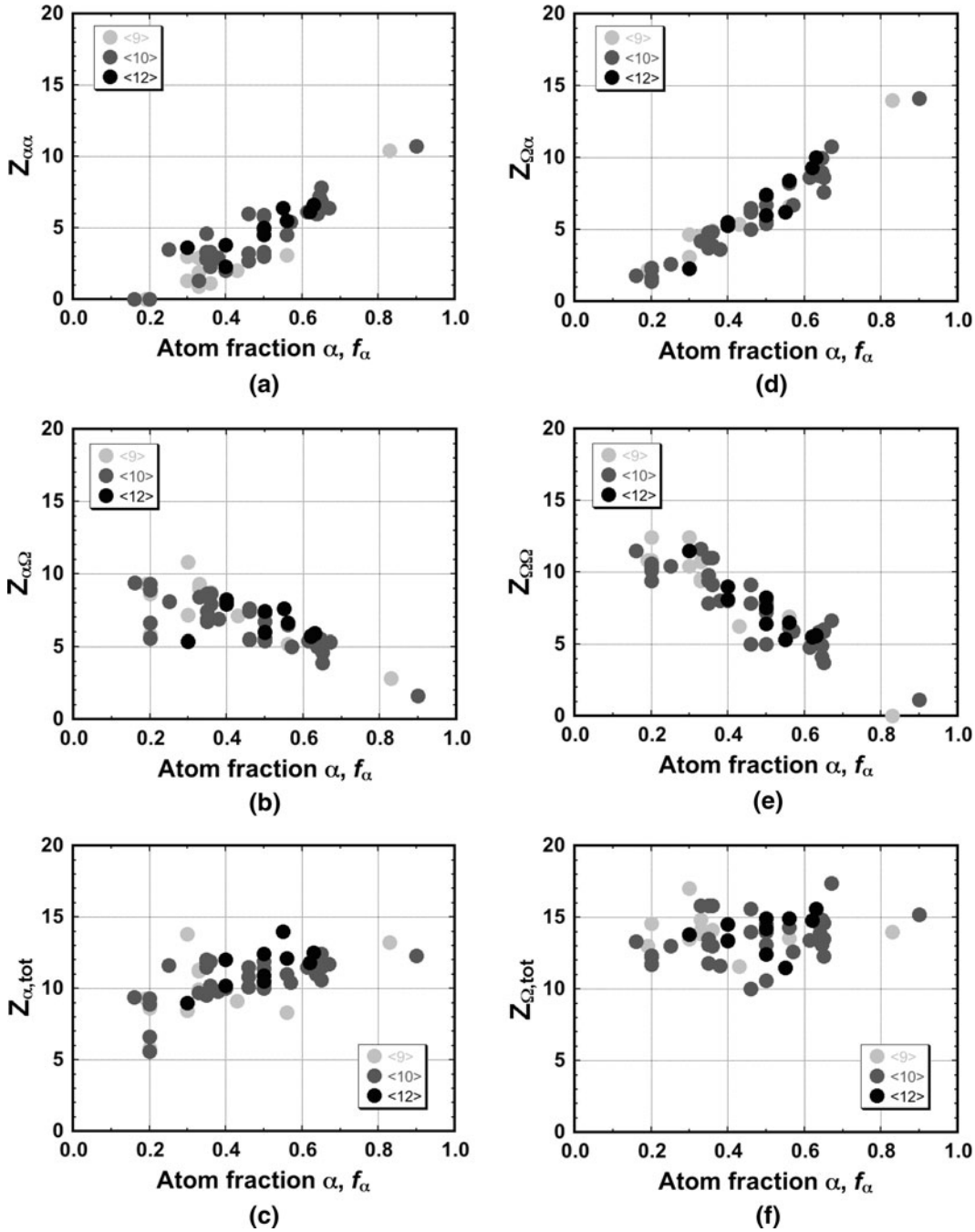

Fig. 1—Measured partial coordination numbers in binary metallic glasses as a function of the atom fraction of the smaller atom. The data are grouped by the relative size of the atoms. Systems with a nominal radius ratio, R, near 0.710 are indicated by <9> (the maximum number of larger atoms that can be first neighbors to a smaller atom), glasses with R near 0.799 are shown as <10>, and glasses with $R \approx 0.902$ are shown as <12>. The α atom is taken to be the smaller atom and Ω is the larger atom. The data are taken from Ref. 8 and from Refs. 5 and 9–11.

given in Table I, and the values with high assessed errors are indicated.

In addition to experimental errors, differences in Z_{ij} could come from systematic structural differences related to relative atom size and quench rate. The magnitude of chemical interactions between the atoms, ε_{ij}, might also influence Z_{ij} through the degree of short-range atomic order.[12] Typically, metallic glasses form in systems with negative heats of mixing, suggesting that the bond energy between unlike atoms is more negative than the average of bond energies between like-atom pairs, $\varepsilon_{\alpha\Omega} < (\varepsilon_{\alpha\alpha} + \varepsilon_{\Omega\Omega})/2$. Bonding between unlike atoms is increasingly preferred as the magnitude of this inequality becomes more negative, thus influencing Z_{ij} values. The largest amount of partial coordination data is available for Zr-Cu and Zr-Ni systems. Cu and Ni atoms are nearly identical in size, and the chemical interactions in these two binary systems are expected to

Distribution Statement A. Approved for public release; distribution unlimited.

Table I. Experimental Z_{ij}: Data are Taken from Ref. 8 Unless Otherwise Noted

Ω	α	f_α	R	$Z_{\alpha\alpha}$	$Z_{\alpha\Omega}$	$Z_{\Omega\alpha}$	$Z_{\Omega\Omega}$	$Z_{\alpha,\mathrm{tot}}$	$Z_{\Omega,\mathrm{tot}}$	Ref.
Ni	B	0.19	0.698	0	9.3	2.2	10.8	9.3	13.0	
Ni	B	0.20	0.698	0	5.8†	1.5	10.8	5.8†	12.3	
Ni	B	0.33	0.698	0.9	9	4.4	9.4	9.9	13.8	
Ni	B	0.36	0.698	1.1	8.7	4.9	9.2	9.8	14.1	
Fe	B	0.20	0.704	0	8.6	2.2	12.4	8.6	14.6	
Y	Cu	0.33	0.704	2.9	8.4	4.1	10.7	11.3	14.8	
Y	Ni	0.33	0.704	1.9	9.3	4.6	9.5	11.2	14.1	
Y	Cu	0.833	0.704	10.4	2.8	14.0	0	13.2	14.0	
Zr	Be	0.43	0.709	2	7.1	5.4	6.2	9.1	11.6	
Dy	Ni	0.30	0.720	1.3	7.2	3.1	10.4	8.5	13.5	
Dy	Ni	0.30	0.720	3†	10.8†	4.6†	12.4†	13.8†	17.0†	
Dy	Ni	0.56	0.720	3.1	5.2	6.6	6.9	8.3	13.5	
Ti	Si	0.16	0.775	0	9.4	1.8	11.5	9.4	13.3	
Pd	Si	0.20	0.775	0	6.6†	1.7	10.6	6.6†	12.3	
Y	Al	0.90	0.788	10.7	1.6	14.1	1.1	12.3	15.2	
Ti	Be	0.38	0.789	2.9	6.9*	3.6*	8	9.8	11.6	
Zr	Ni	0.33	0.797	1.3	8.4	4.2	11.6	9.7	15.8	
Zr	Cu	0.35	0.797	4.6	6.9	3.7	9.4	11.5	13.1	10
Zr	Cu	0.35	0.797	4.6	7.4	4.0	7.8	12	11.8	
Zr	Cu	0.35	0.797	2.8	6.7*	3.7*	9.8	9.5	13.5	
Zr	Ni	0.35	0.797	3.3	8.6*	4.8*	11	11.9	15.8	
Zr	Ni	0.36	0.797	2.3	7.9*	3.9*	9.1	10.2	13	
Zr	Ni	0.36	0.797	3.3	8.6	4.8	11	11.9	15.8	
Zr	Cu	0.40	0.797	2.0	8.0	5.4	8.0	10.1	13.4	5
Zr	Cu	0.455	0.797	2.7	7.4	6.2	7.8	10.1	14.0	5
Zr	Cu	0.46	0.797	6.0	5.5	5.0†	5†	11.5	10†	
Zr	Cu	0.46	0.797	3.2	7.6	6.5	9.1	10.8	15.6	9
Zr	Cu	0.50	0.797	5.9	6.0	6.0	8	11.9	14	10
Zr	Cu	0.50	0.797	5.8	5.6	5.6	5	11.4	10.6	
Zr	Cu	0.50	0.797	4.9	5.4	5.4	7.7	10.3	13.1	
Zr	Cu	0.50	0.797	3.0	7.3	7.3	7.2	10.3	14.4	5
Zr	Ni	0.50	0.797	3.3	6.7	6.7	7.8	10	14.5	
Zr	Cu	0.56	0.797	4.5	6.5	8.2	6.1	11.0	14.3	5
Zr	Cu	0.57	0.797	5.4	5.0*	6.7*	5.9	10.4	12.6	
Zr	Cu	0.614	0.797	6.1	5.4	8.6	4.8	11.5	13.3	5
Zr	Ni	0.637	0.797	6.0	5.0	8.8	5.8	11	14.6	
Zr	Ni	0.64	0.797	6.0	5.0	8.9	5	11	13.9	
Zr	Cu	0.645	0.797	6.3	5.5	9.9	4.9	11.7	14.8	11
Zr	Cu	0.645	0.797	7.2	4.9	9.0	4.1	12.1	13.1	5
Zr	Cu	0.65	0.797	7.8	4.6	8.6	6	12.4	14.6	10
Zr	Cu	0.65	0.797	6.9	4.6	8.6	3.7	11.5	12.3	
Zr	Cu	0.65	0.797	6.7	3.9*	7.6*	5.9	10.6	13.5	
Zr	Ni	0.67	0.797	6.4	5.3	10.8	6.6	11.7	17.4	
Ni	P	0.20	0.810	0	9.3	2.3	9.4	9.3	11.7	
Co	P	0.20	0.816	0	8.9	2.2	10.1	8.9	12.3	
Fe	P	0.25	0.816	3.5	8.1*	2.6*	10.4	11.6	13	
Pt	Ge	0.20	0.820	0	5.6†	1.4	10.3	5.6†	11.7	
Ta	Ni	0.50	0.869	4.9	6	6	8.2	10.9	14.2	
Ta	Ni	0.55	0.869	6.4	7.6*	6.2*	5.3	14	11.5	
Nb	Ni	0.40	0.881	3.8	8.2	5.5	9	12	14.5	
Nb	Ni	0.50	0.881	5	7.4	7.4	7.5	12.4	14.9	
Nb	Ni	0.56	0.881	5.5	6.6	8.4	6.5	12.1	14.9	
Nb	Ni	0.62	0.881	6.1	5.7	9.3	5.5	11.8	14.8	
Nb	Ni	0.63	0.881	6.6	5.9	10	5.6	12.5	15.6	
Ti	Cu	0.50	0.887	4.5	6	6	6.4	10.5	12.4	
Ti	Ni	0.40	0.887	2.3	7.9	5.3	8.1	10.2	13.4	
Zr	Pd	0.30	0.899	3.6†	5.4†	2.3	11.5	9.0†	13.8	

*Data do not satisfy required identity in Eq. [1].
†Deviates by at least 3 from values expected for efficient topological packing.

be roughly similar based on the similar electronegativities, compound formation, and melting temperatures in these two systems. Thus, the data from these two binaries might reduce systematic variations in Z_{ij} because of topology and chemical effects. Nevertheless, data from the Zr–Ni and Zr–Cu binary systems still

Distribution Statement A. Approved for public release; distribution unlimited.

show essentially the same degree of scatter (Figure 2) as for the full data set and suggest that an error in Z_{ij} of ± 1 is typical and may be as large as ± 1.5.

Despite significant scatter, clear trends are observed. As expected, increasing f_α gives higher $Z_{\alpha\alpha}$ and $Z_{\Omega\alpha}$, and decreases $Z_{\alpha\Omega}$ and $Z_{\Omega\Omega}$ systematically. The maximum values of $Z_{\alpha\alpha}$ and $Z_{\Omega\Omega}$ both approach approximately 12. Within experimental error, $Z_{\alpha\alpha}$ is 0 for $f_\alpha \leq 0.2$ and $Z_{\Omega\Omega}$ is 0 for $f_\alpha \geq 0.8$ as expected in systems where solute–solute contact is avoided, as suggested by the ECP model.[6,7] The maximum values for $Z_{\alpha\Omega}$ approach ~9 to 12 as f_α approaches 0, and the maximum in $Z_{\Omega\alpha}$ approaches ~15 to 17 as f_α approaches 1. Finally, the total coordination around α ranges from approximately 9 or 10 when f_α is small to about 12 or 13 as f_α approaches 1, whereas the total coordination around Ω varies from approximately 12 or 13 when f_α is small to values 15 or higher as f_α approaches 1.

Although these trends match simple expectations, currently no convenient approach is available to estimate Z_{ij} in metallic glasses that accounts for relative atom size and atom fraction. These values can be determined with confidence in atomic simulations, but simulations require high-fidelity atomic potentials that

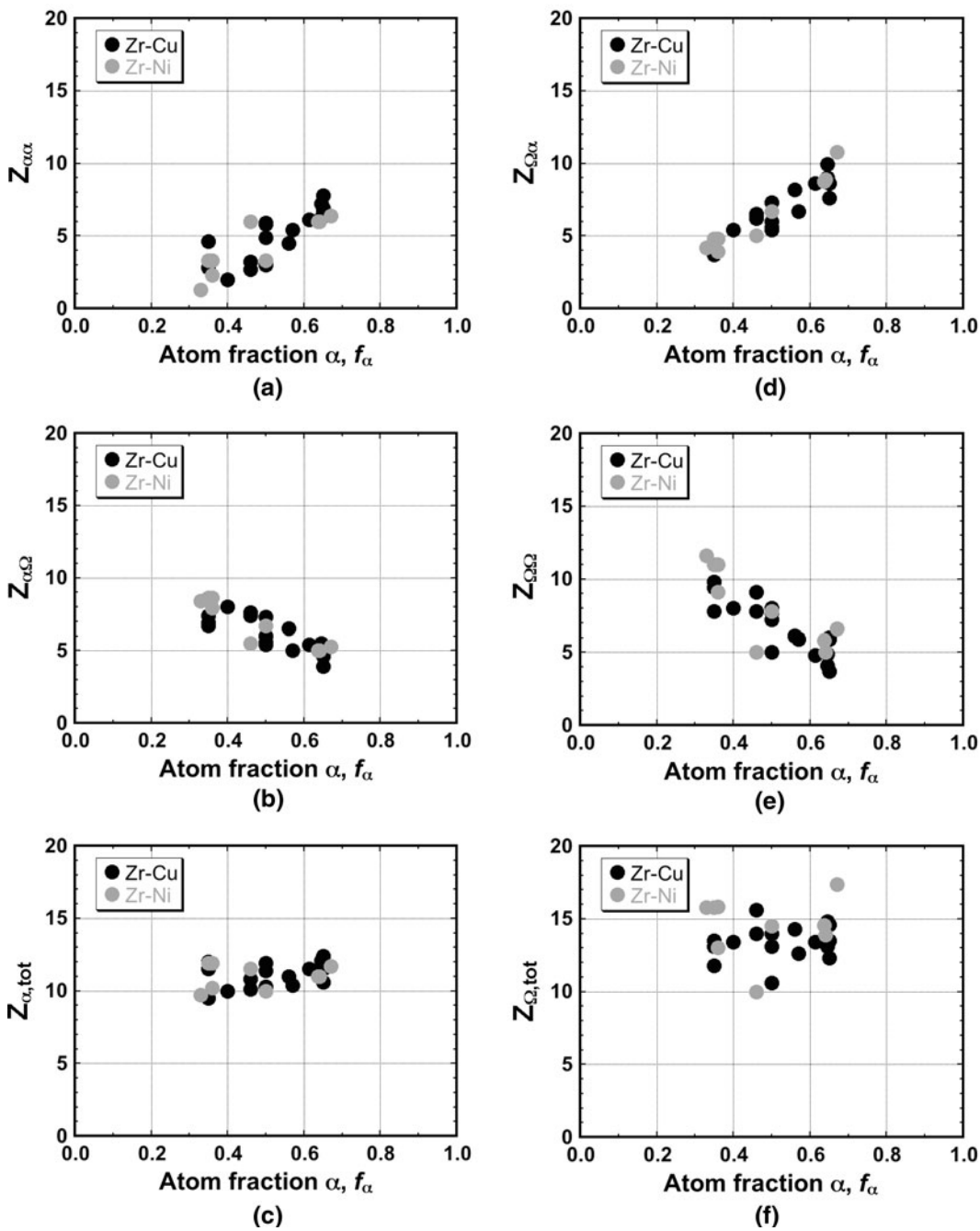

Fig. 2—Measured partial coordination numbers in binary Zr-Cu and Zr-Ni metallic glasses. All are <10> glasses with a nominal radius ratio of 0.797. The data are taken from Ref. 8 and from Refs. 5 and 9–11.

Distribution Statement A. Approved for public release; distribution unlimited.

are difficult to produce and validate. A relative lack of high-quality atomic potentials makes it difficult to use simulations to identify trends across many systems with a broad range of topologies and chemistries. A recent effort estimates Z_{ij} in binary systems by including effects of chemical short-range ordering into cluster-packing models via a quasi-chemical-type approach.[12] This gives good agreement with experimental data and gives an average difference from measured partial coordination numbers of 0.76, which is a slightly better than an average difference of 0.82 obtained from a simple topological approach that does not include chemical effects (note typographical errors in the text and Table III of Reference 12 regarding ECP predictions). However, this approach requires data that are not widely available. The ECP model gives an approach for estimating Z_{ij} and has been applied successfully to many systems.[7] However, agreement is best for solute-lean glasses, where the relative atomic size and solute concentrations are such that each solute can have solvent atoms only as first neighbors. Simplifications in the approach for estimating Z_{ij} from the ECP model gave a less compelling agreement for solute-rich glasses, where solute–solute contact is unavoidable. As the most stable glasses are almost always solute rich,[8] extending a predictive capability to solute-rich glasses would give an important new capability.

The objective of the current work is to develop a topological approach for estimating partial coordination numbers in binary metallic glasses and to apply this to a broad range of binary metallic glasses. An explicit account of the relative atomic size and atom fraction is included, and calculations are developed over the full composition range so that solute-rich glasses are covered. Predictions are compared with experimental data. The trends in Z_{ij} as a function of relative atomic size and composition are analyzed to explore experimental scatter and to look for new insights into the structure of solute-rich glasses.

II. DEFINITION OF STRUCTURAL TERMS

Structure-specific equations that account for composition and relative atomic size are developed for the four Z_{ij} values in binary metallic glasses. Structural terms that include topological information are taken from the ECP model.[6–8] These terms are introduced briefly and described for metallic glasses consisting of α solute atoms and Ω solvent atoms.

The ECP model allows the sites in a metallic glass structure to be counted. For each α site in the structure, there is 1 β site, 2 γ sites, and $\hat{S}_\Omega$ Ω sites, so that the total number of structural sites per α site is $(\hat{S}_\Omega + 4)$. $\hat{S}_\Omega$ ranges from 8 to 20 and depends on the nominal radius ratio $R = r_\alpha / r_\Omega$ of solute and solvent atoms.[13] The ECP model also allows the occupancy of sites in a metallic glass structure to be specified. Ω atoms only occupy Ω sites, but α atoms can occupy any site in the structure. α and Ω sites are always occupied, but β and γ sites can be occupied by α or can be vacant. The α atoms first occupy α sites, followed by β sites, then γ sites, and finally Ω sites as the solute atom fraction increases.

The glass is solute lean when the number of α atoms is insufficient to fill all α, β, and γ sites, and the solute atom fraction f_α is given as

$$f_\alpha = \bar{S}_\alpha / (\hat{S}_\Omega + \bar{S}_\alpha) \quad [2a]$$

where $\bar{S}_\alpha$ is the total number of α atoms in the structure normalized by the number of α sites. In solute-lean glasses, $\bar{S}_\alpha \leq 4$. Rearranging terms gives $\bar{S}_\alpha$ as a function of f_α for solute-lean glasses

$$\bar{S}_\alpha = \hat{S}_\Omega \left(\frac{f_\alpha}{1 - f_\alpha} \right) \quad [2b]$$

In solute-rich glasses, there are enough α atoms to fill all α, β and γ sites and some of the Ω sites. In these structures,

$$f_\alpha = \bar{S}_\alpha / (\hat{S}_\Omega + 4) \quad [3a]$$

so that

$$\bar{S}_\alpha = f_\alpha (\hat{S}_\Omega + 4) \quad [3b]$$

In solute-lean glasses, $\hat{S}_\Omega$ is constant. However, $\hat{S}_\Omega$ changes with composition in solute-rich glasses as Ω sites are filled progressively by α atoms.[8] If α is smaller than Ω, then $\hat{S}_\Omega$ increases with increasing f_α, and $\hat{S}_\Omega$ decreases with increasing f_α when α is larger than Ω. This is accounted for through an effective radius of atoms on Ω sites, $\tilde{r}_\Omega$

$$\tilde{r}_\Omega = r_\alpha \left(\frac{S(\alpha_\Omega)}{\hat{S}_\Omega} \right) + r_\Omega \left(1 - \frac{S(\alpha_\Omega)}{\hat{S}_\Omega} \right) \quad [4]$$

where $S(\alpha_\Omega)$ is the number of α atoms on Ω sites normalized by the number of α sites. In this weighted average, $(S(\alpha_\Omega)/\hat{S}_\Omega)$ is the fraction of Ω sites occupied by α and $(1 - S(\alpha_\Omega)/\hat{S}_\Omega)$ is the fraction of Ω sites occupied by Ω. $S(\alpha_\Omega) = 0$ in solute-lean glasses and $S(\alpha_\Omega) = (\bar{S}_\alpha - 4)$ in solute-rich glasses. The influence of atom size and composition is obtained by using an effective radius ratio $\tilde{R} = r_\alpha / \tilde{r}_\Omega$ in the equation for $\hat{S}_\Omega$ [see Eq. [7] in Reference 13]. Because $\hat{S}_\Omega$ depends on $\tilde{R}$ and because $\tilde{R}$ depends on $\hat{S}_\Omega$, an iterative solution for $\hat{S}_\Omega$ and $\tilde{R}$ is required.[8] The terms f_α, R, $\hat{S}_\Omega$, $\bar{S}_\alpha$, and $S(\alpha_\Omega)$ are evaluated elsewhere for all binary metallic glasses.[8]

The term $\hat{S}_\Omega^{R=1}$ is used to indicate the maximum number of Ω atoms that is possible in the first shell of another Ω atom. This is determined by setting $R = 1$ in the equation for $\hat{S}_\Omega$, which gives a value of 13.33. This falls between the maximum number of unit spheres that can simultaneously contact a central unit sphere (12) and the number of first-neighbors in a body-centered cubic structure using a Voronoi definition of coordination number (14), where 8 atoms in the first shell contact the central atom, and the remaining 6 atoms are at a distance approximately 15 pct larger than the minimum separation. The value $\hat{S}_\Omega^{R=1} = 13.33$ is used in the

Distribution Statement A. Approved for public release; distribution unlimited.

following analyses to acknowledge that all the atoms in the first coordination shell do not need to contact the central atom, and some coordinating atoms may be slightly displaced from contact. This is also consistent with the approach commonly used in experiments, where atoms are considered as first neighbors up to the first minimum in the radial distribution function, which often occurs at approximately 125 pct of the minimum atomic separation.

The terms "α" and "solute" have thus far been used interchangeably and are taken as the minority species. However, as f_α increases, the structure will eventually become an α-based glass with Ω atoms as the minority species. This transition occurs at the isostructural composition $f_{\text{iso.}}$[8] When the α and Ω atoms are of equal size, $f_\alpha = 0.50$. However, the number of structural sites in metallic glasses depends on the relative sizes of α and Ω. A smaller α is structurally less potent because it produces fewer Ω sites. As a result, f_{iso} is greater than 0.50 when $R < 1$ and is less than 0.50 when $R > 1$. In developing equations for Z_{ij}, the terms solute and solvent will be used for the structural minority and majority species, respectively.

III. CALCULATION OF Z_{IJ}

It is assumed that efficient atomic packing occurs locally around both solute and solvent atoms, as supported by phenomenological correlations[1] and previous calculations.[2] A statistical approach is used to develop the Z_{ij} equations from the product of four terms: (1) the number of reference sites occupied by an i atom normalized by the number of α sites in the structure, (2) the probability of finding an i atom at that site, (3) the number of structural sites occupied by a j atom that contact the i site, and (4) the probability of finding a j atom at this site. This product gives the total number of i–j contacts. To get Z_{ij}, the number of contacts is normalized by the number of i atoms in the system considered. A more detailed description of the Z_{ij} equations is given in the Appendix.

Partial coordination numbers are calculated from Eqs. [A4] through [A10] for binary systems with nominal radius ratios of $R = 0.710$, 0.799, and 0.902. These equations are applied from the minimum solute concentrations needed to form a glass (see Eq. [2a], where $\bar{S}_\alpha = 1$) up to f_{iso} (0.60 for $R = 0.710$; 0.57 for $R = 0.799$ and 0.53 for $R = 0902$). When $f_\alpha > f_{\text{iso}}$, the calculations are performed for the inverse systems, where α becomes the solvent and Ω becomes the solute. Thus, the nominal radius ratio in the inverse system R^{-1} is given by $1/R = r_\Omega/r_\alpha$ and the solute atom fraction in the inverse system is $f_\alpha^{-1} = 1 - f_\alpha$. Other parameters in Eqs. [A4] through [A10] are transformed accordingly. To avoid confusion and to enable visualization of the trends across f_{iso} while maintaining a consistent notation, the experimental Z_{ij} values in Table I and the calculated Z_{ij} values in the following figures report α as the smaller atomic species over the full range of f_α.

The effective radius ratio (ERR) gives a second approach to estimate Z_{ij} based on the assumption that a global alloy composition can be represented by the atomic composition of an i-centered atomic cluster, with a small "stoichiometric remainder"[1] or "glue atoms"[14] as required. Again, efficient local atomic packing is assumed, and the effective radius ratio $\tilde{R} = r_\alpha/\tilde{r}_\Omega$ described previously is used to define preferred local cluster coordination at integer values of Z, i, and j. Equations [A12] through [A17] describe the ERR calculation to generate partial and total coordination numbers using an ideal packing efficiency normalization and linear extrapolation between the two bounding, efficiently packed i- or j-centered clusters as a function of f_α.

IV. RESULTS AND DISCUSSION

The results are plotted with the experimental data in Figure 3. For clarity, Z_{ij} data with large assessed errors (Table I) are omitted from this comparison. Predictions from both approaches generally match the experimental trends and reproduce measured data within the assessed experimental error of ±1.5. The calculated values satisfy Eq. [1] and match across f_{iso}, giving additional confidence in the estimates. Chemical effects are expected to influence the local atomic structure, and detailed approaches such as that of Lass *et al.*[12] are expected to be useful. However, the current results show that topology alone gives a good representation of the data, suggesting that the magnitude of chemical effects on Z_{ij} values may be within experimental scatter.

The development of equations for Z_{ij} from the ECP model uses a statistical view of topology, and the Z_{ij} values calculated here are global averages. In the ECP approach, the same type of atom can have different Z_{ij} values when occupying different sites. For example, in the same structure, the number of α atoms around an α atom that occupies an α site can be different than the number of α atoms around an α atom that occupies an Ω site. The differences are not large. For example, in solute-rich glasses with a nominal R of 0.799 and $S(\alpha_\Omega) = 2$, $Z_{\alpha\alpha}$ is 2 for α atoms on α sites and is 1.9 for α atoms on Ω sites. At a higher f_α, so that $S(\alpha_\Omega) = 7$, $Z_{\alpha\alpha}$ is 7 for α on α sites and is 5.9 for α on Ω sites. Similar differences are found for $Z_{\alpha\Omega}$ and $Z_{\Omega\alpha}$ in solute-rich glasses. No other site-specific differences in Z_{ij} are indicated by Eqs. [A4] through [A10] in the Appendix.

The ERR approach gives cluster compositions that correspond closely to the bulk alloy composition, where efficient local atomic packing is obtained with an integral number of constituent atoms in the first coordination shell. A strong correlation is found between these compositions and glass-forming ability, suggesting that these efficiently packed i- or j- centered clusters may be statistical representatives of majority structural elements of the glass.[1] Although the ERR approach implicitly assumes that the first-neighbor environments around a given species are equivalent, it remains to be shown that, for example, the coordination shell of an efficiently packed, α-centered cluster is identical to the first-neighbor environment of an α atom in the first shell of such a cluster. Even if this is found to

Distribution Statement A. Approved for public release; distribution unlimited.

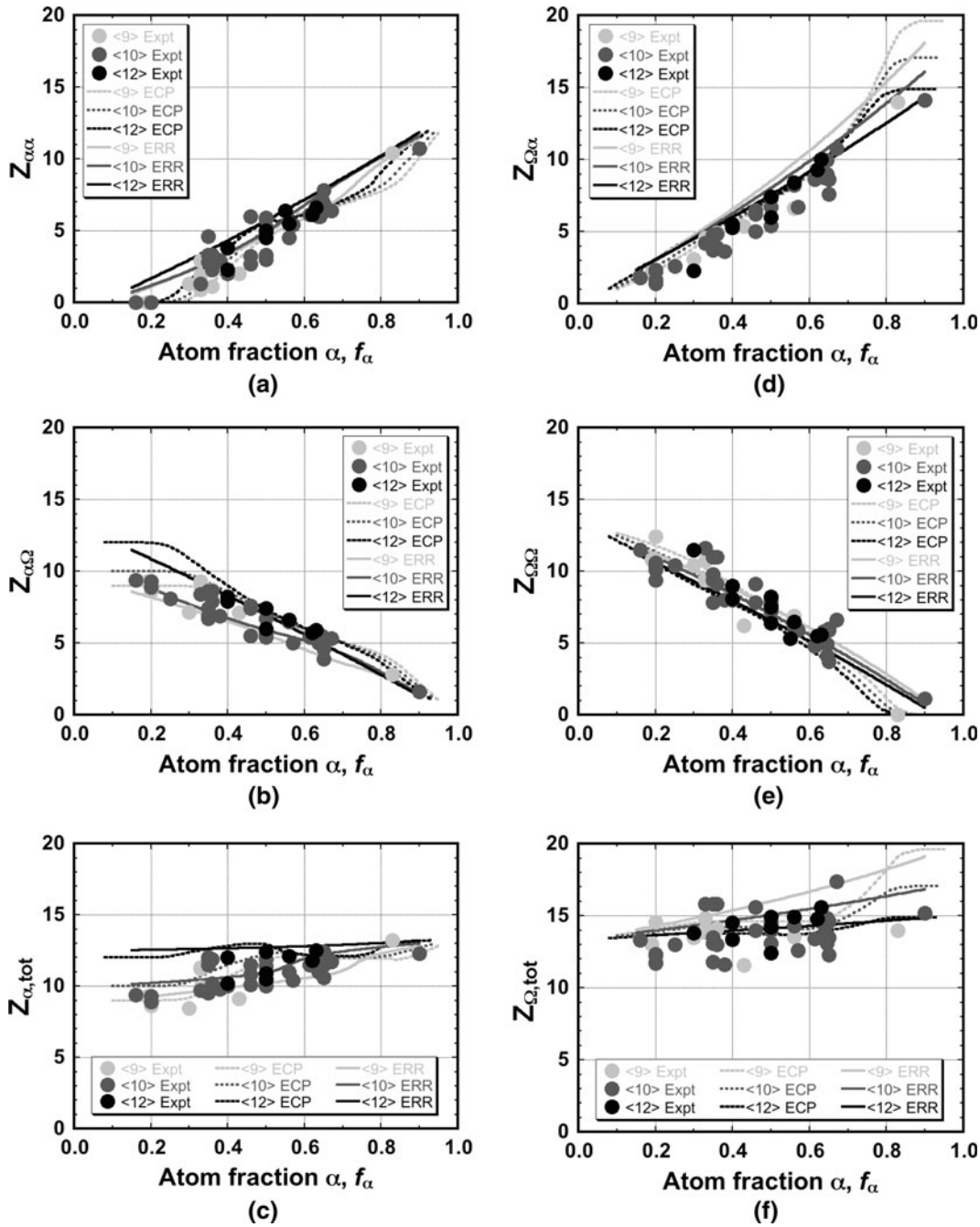

Fig. 3—Calculated partial coordination numbers in binary metallic glasses compared with experimental data. The experimental data are taken from Ref. 8 and from Refs. 5 and 9–11.

be true, the condition where first-neighbor environments are identical for a given species throughout the structure applies only to discrete compositions. For most compositions, the structure consists of efficiently packed clusters with a stoichiometric remainder of atoms or a mixture of more than one type of efficiently packed clusters. Currently, there is no way to estimate the first-neighbor environment of the stoichiometric remainder, and there is no reason to expect that the first shell of these atoms will be identical to the other atoms. Thus, a given glass structure may have a range of first-neighbor environments with local Z_{ij} values that vary slightly from the global average Z_{ij} values.

From the previous discussion, Z_{ij} values from both the ECP and ERR approaches suggest that small, local variations in first-neighbor environments are expected. This is consistent with the concept of quasi-equivalent clusters,[15] where distributions in first-neighbor environments are shown in atomistic simulations. This gives topological fluctuations in both local constitution and packing that are expected to be important.[16]

Distribution Statement A. Approved for public release; distribution unlimited.

Predictions for $Z_{\Omega\alpha}$ from the ECP model diverge from experimental data when $R < 1$ and $f_\alpha > f_{iso}$. This represents structures where the larger Ω atoms are surrounded increasingly by the smaller α atoms. These structures can be viewed equivalently as solute-lean glasses with $R > 1$, where larger solute atoms are surrounded by smaller solvent atoms. Like glasses with $R < 1$, these solutes are expected to occupy α, β, and γ sites progressively as the atom fraction of the larger solute atoms increases. The smaller experimental $Z_{\Omega\alpha}$ values suggest that contact between larger atoms occurs at lower concentrations than predicted by the ECP model, so that the larger atoms might not occupy β and γ sites. To explore this possibility, the sizes of β and γ sites are estimated in the Appendix as a function of the solute size and are plotted in Figure 4(a). Although the sizes of β and γ sites show significant variability because of the nonspherical nature of the clusters, in general the β sites can accommodate α atoms up to $R \approx 1.12$. When solute atoms are larger than this, the α atoms can no longer be placed in β sites without pushing apart the constituent clusters. This is illustrated in Figure 4(b), where a solute with $R < 1$ fits in a β site but a solute with $R > 1$ overlaps atoms in the bounding clusters. In contrast, the γ sites are too small to hold α atoms without increasing the cluster–cluster separation over the full range of α atom sizes. Figure 4(a) suggests that filling γ sites with α solutes will produce increasingly larger strains between structure-forming clusters with increasing R.

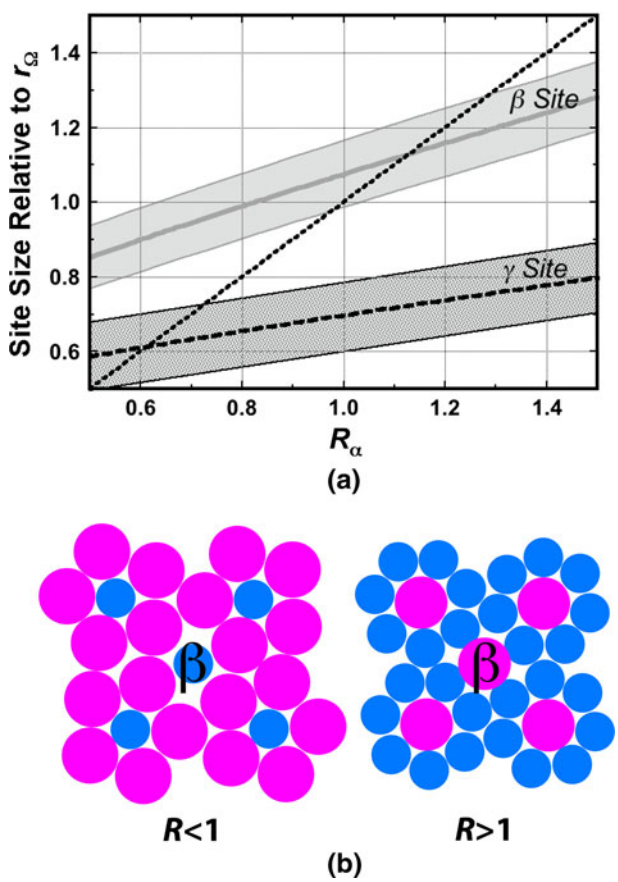

Fig. 4—(*a*) Estimated size (see Appendix) of atoms that can fit into β and γ sites without forcing clusters apart. The lower bounds for the β site and γ site bands are for face contact, the upper bounds are for edge contact, and the centerline is a simple average of these two bounds. The dotted line represents the condition where the site size is exactly equal to the size of the α atom. R_α and the solute site sizes are both relative to the radius of Ω atoms, r_Ω. (*b*) Illustration showing the size of β sites relative to the size of the solutes. When $R < 1$, the solute can fit into β sites, but when $R > 1$, the solute is too large to fit in β sites without pushing apart the bounding clusters.

Experimental evidence gives clues to the site-filling sequence in metallic glasses and supports this suggestion that α occupancy of γ sites increases cluster–cluster separation. Diffraction results show that α–α contact does not occur in any glass when $R < 1$ and $f_\alpha < 0.30$ (Table I), demonstrating a remarkable tendency for solute atoms to avoid contact. In the ECP model, this avoidance is accomplished by filling α, β, and γ sites between solute-centered clusters with solvent atoms only in the first shells. Because Ω sites surround α, β, and γ sites, solute–solute contact can only occur when α atoms occupy Ω sites. Solute–solute contact becomes unavoidable when $R < 1$ and $f_\alpha \geq 0.30$, after the α, β, and γ sites are fully occupied and additional solute atoms must occupy Ω sites. Consistent with this, the data in Table I show that solute–solute contact occurs in every glass where $f_\alpha \geq 0.30$. Additional support for the filling and relative sizes of β and γ sites is given by density measurements in melt-quenched Fe-B metallic glass ribbons. The density is relatively insensitive to concentration from boron atom fractions of 0.13 to approximately 0.19, and the density drops linearly from boron atom fractions of approximately 0.19 to 0.27.[17] In Fe-B, the β sites are fully occupied ($\bar{S}_\alpha = 2$) between $f_\alpha = 0.18$ and $f_\alpha = 0.19$ (Table A1 in Reference 8), and the decreasing density at higher boron atom fractions is consistent with the idea that the structure-forming clusters are pushed apart as soon as boron begins to fill γ sites.

The most stable Fe-B glasses have a boron atom fraction in the range of 0.18 to 0.20, so that the internal strains and free volume associated with filling of γ sites may contribute to the decreased stability. Nevertheless, nearly three quarters of the γ sites are filled by boron before Fe-B glasses can no longer be made. These observations support the concept that α, β, γ, and Ω sites are filled progressively by solutes with increasing f_α in structures with $R < 1$, and that solute occupancy of β sites does not distort the structure while solute occupancy of γ sites introduces a structural expansion.

Only two Z_{ij} data sets are available for solute-lean glasses with $R > 1$ (see Table I for glasses with $R < 1$ and $f_\alpha > 0.79$), and the values are ambiguous regarding avoidance of solute–solute contact. Y-Y contact is absent in $Y_{0.167}Cu_{0.833}$ at a composition that suggests that Y fills α, β, and γ sites, whereas $Z_{YY} = 1.1$ in $Y_{0.10}Al_{0.90}$ at a composition where the Y fills only α and β sites. Errors in Z_{YY} from $Y_{0.10}Al_{0.90}$ are estimated to be ±50 pct as a result of counting statistics,[18] and additional errors are expected from the assumed atomic radii used to fit the data.[2] No data are available for glasses with $R > 1$ between the solute atom fractions of $0.167 \leq f_\alpha \leq 0.33$ (see Table I for glasses with $R < 1$ and $0.67 \leq f_\alpha \leq 0.833$). However, the site-filling sequence can be inferred from Figure 5, which shows that most

Distribution Statement A. Approved for public release; distribution unlimited.

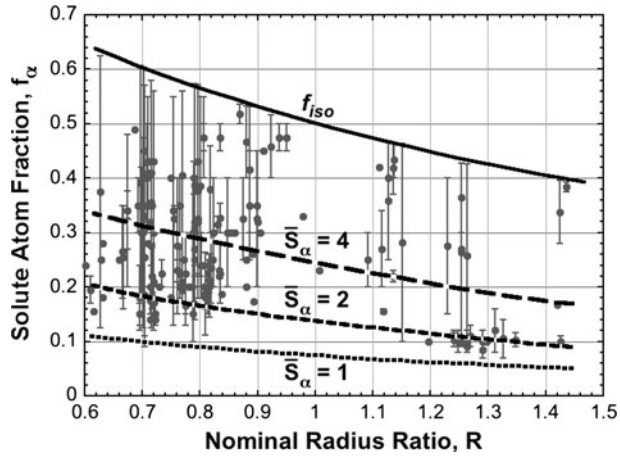

Fig. 5—Topologies (relative sizes and concentrations) for all binary metallic glasses showing a preference for metallic glasses with $R < 1$. Most binary glasses with $R > 1.26$ have solute atom fractions suggesting that α and β sites, but not γ sites, are occupied by solutes ($\bar{S}_\alpha \leq 2$). Redrawn from Figure 5 in Ref. 8.

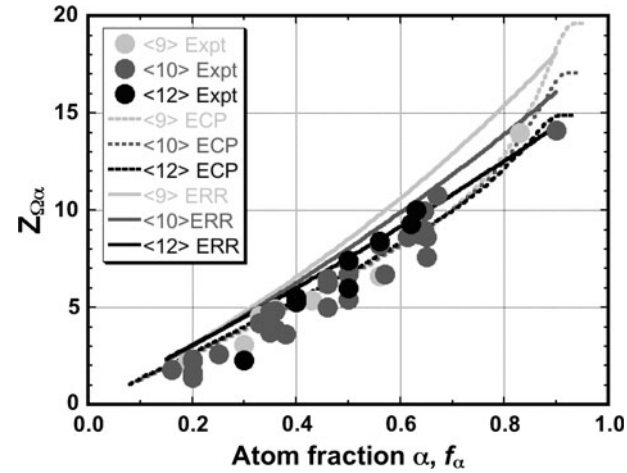

Fig. 6—Calculated $Z_{\Omega\alpha}$, modified to account for the inability to fill γ sites in glasses with $R < 1$ and $f_\alpha > f_{iso}$, compared with experimental data. The experimental data are taken from Ref. 8 and from Refs. 5 and 9–11.

known binary metallic glasses have $R < 1$. These glasses occur over the full range of solute atom fractions, and the discussion supports the view that α, β, γ, and Ω sites are filled progressively as f_α increases. Binary glasses with $1 \leq R \leq 1.26$ are also often solute rich ($\bar{S}_\alpha > 4$), suggesting that solutes occupy α, β, γ, and Ω sites in these glasses as well. In contrast, almost all binary glasses with $R > 1.26$ are solute lean, with solute atom fractions that allow only α and β sites to be filled by solutes ($\bar{S}_\alpha \leq 2$). This suggests that only α and β sites are filled in binary glasses with $R > 1.26$, and that expansion caused by placing larger solutes on γ sites destabilizes the amorphous structure. This gives a structural asymmetry that can explain the observed preference for binary glasses with $R < 1$ and represents an important modification to the ECP model.

This change in site filling can be modeled by a simple modification in the equations used to predict Z_{ij}. Because the divergence applies to values of $Z_{\Omega\alpha}$ in glasses where $R < 1$ and $f_\alpha > f_{iso}$, the equations for $Z_{\alpha\Omega}$ are modified for glasses where $f_\alpha < f_{iso}$ and $R > 1$. Equation [A8] is unchanged but is valid only to $\bar{S}_\alpha \leq 2$ to reflect the change in the boundary between solute-lean and solute-rich structures. This same change is applied in Eq. [A9] by replacing all of the 4s with 2s. The predictions from this simple modification show better agreement with experiment (compare Figure 6 with Figure 3(d)).

From the ERR approach, the structure can be defined also by efficiently packed clusters with mixed first-shell occupancy and only a relatively small number of additional atoms as a stoichiometric remainder between these clusters. Currently, there is no analysis for determining whether the ERR and ECP structures are essentially identical or for distinguishing between these possibilities. Although based on ECP concepts, the ERR approach differs in two major ways: (1) It allows solute–solute contact by assigning the first addition of a solute atom beyond the minimum concentration needed to form solute-centered clusters to the first shell of the structure-forming clusters, and (2) it does not account specifically for intercluster sites such as β and γ sites. A shortcoming of this technique is that at lower solute contents where, by thermodynamics, solute–solute contact is avoided, the ERR method overpredicts the first neighbor solute–solute coordination contribution. Neither the ERR nor the ECP models specify the arrangement of atoms within the coordination shell.

The current equations predict the partial coordination numbers to within experimental scatter, but they are rather cumbersome and require additional calculations to convert f_α to structure-specific ECP parameters or require the consideration of many permutations of possible atomic clusters. As an aid, simple phenomenological equations to estimate the partial coordination numbers of binary metallic glasses as a function of composition and relative atom size are offered in this study. As a function of f_α only, the equations are

$$Z_{\alpha\alpha} = 14.8 f_\alpha - 2.8 \quad [5a]$$

$$Z_{\alpha\Omega} = 11.3 - 9.8 f_\alpha \quad [5b]$$

$$Z_{\Omega\alpha} = 16.8 f_\alpha - 1.7 \quad [5c]$$

$$Z_{\Omega\Omega} = 14.2 - 14.1 f_\alpha \quad [5d]$$

Both f_α and R are accounted for independently in the phenomenological equations

$$Z_{\alpha\alpha} = 14.57 f_\alpha + 2.79 R - 4.91 \quad [6a]$$

$$Z_{\alpha\Omega} = -9.91 f_\alpha + 1.37 R + 10.26 \quad [6b]$$

$$Z_{\Omega\alpha} = 16.90 f_\alpha - 1.47 R - 0.53 \quad [6c]$$

$$Z_{\Omega\Omega} = -14.28 f_\alpha + 2.32 R + 12.43 \quad [6d]$$

Distribution Statement A. Approved for public release; distribution unlimited.

These simple phenomenological equations predict Z_{ij} within experimental scatter, and the squared linear regression correlation coefficients range from 0.85 to 0.94 for all equations. The equations for $Z_{\alpha\alpha}$ and $Z_{\Omega\Omega}$ are undefined for values less than zero, and the equations for $Z_{\alpha\Omega}$ and $Z_{\Omega\alpha}$ are undefined for values less than one.

V. CONCLUSIONS

The equations for partial coordination numbers in binary metallic glasses Z_{ij} are derived from statistical topology and the requirement of efficient local atomic packing. Two related topological models are used, the ECP model and the ERR model. The equations from both ECP and ERR topologies give a good ability to estimate systematic trends in Z_{ij} as a function of relative atomic size and composition. The estimates are typically accurate to within the assessed experimental scatter of ± 1.5, validating the underlying structural concepts. Although expected to be important, the magnitude of a chemical influence on local atomic structure is less than the current experimental scatter. Deviations from experimental data suggest improvements in the ECP and ERR structural topologies. The ECP model overestimates $Z_{\Omega\alpha}$ when the atom fraction of α approaches 1, leading to the observation that β sites can accommodate α solutes up to $R < 1.12$, but an expansion of bounding clusters is needed to place α solutes in β sites when $R > 1.12$. γ sites are always smaller than α solutes, so that it is increasingly difficult to place α solutes in γ sites as solute size increases. Observed glass topologies and estimates of the sizes of β and γ structural sites in the ECP model suggest that γ sites are not occupied when $R > 1.26$. Modified equations give an improved match with experimental data when this topological anomaly is considered. This important modification gives an asymmetry to the site-filling rules of the ECP model and explains a preference for glasses with $R < 1$. The current application of the ERR model does not account for overlapping structure-forming clusters, and hence, it does not accommodate the experimentally observed tendency to avoid solute–solute contact for solute-lean metallic glasses. Simplified empirical equations for Z_{ij} are given for convenience.

ACKNOWLEDGMENTS

This work was supported by a grant from the Air Force Office of Scientific Research (M. Berman, Program Manager, Grant Number 10RX14COR). K.J.L. acknowledges a Window on Science grant from the Asian Office of Aerospace Research and Development (Dr. K. Jata, Program Manager).

APPENDIX

An accounting of all possible contacts in a glass system can be summarized by the equation

$$Z_{ij} = \frac{S_1 p_1 S_2 p_2 + S_3 p_3 S_4 p_4 + S_5 p_5 S_6 p_6}{m} \qquad [A1]$$

where S_n and p_n are the number of reference sites and their probability of occupancy, whereas m is the number of reference atoms of interest. For consistency across Z_{ij}, all S_n refer to the same site in all cases; S_1 describes the occupancy of α sites, whereas S_2 describes the species occupying the Ω sites coordinated around that α site. S_3 describes the occupancy of the Ω sites, whereas S_4 describes the occupancy of α sites coordinated around that Ω. Likewise, S_5 describes the occupancy of the Ω sites, whereas S_6 describes the occupancy of Ω sites around an Ω. Using this approach, two relationships are developed for each Z_{ij}: one for solute-lean glasses ($\bar{S}_\alpha \leq 4$) and one for solute-rich glasses ($\bar{S}_\alpha > 4$). Table AI lists the values of S_n and p_n for each case of interest.

As an example, consider $Z_{\alpha\alpha}$ for the solute-rich case where α–α contact can occur three different ways: from an α atom on a solute site to an α atom on an Ω site, from an α atom on an Ω site to an α atom on a solute site, and from one α atom on an Ω site to another α atom on a different Ω site. Because solute sites are always separated by Ω sites, there is no α–α contact between solute sites. Starting with the first of these terms, we define values for each of the four terms (1) through (4) described previously that correspond to S_1,p_1,S_2, and p_2, respectively. On average, four solute sites contact each Ω site (S_1), and the probability of these sites being occupied by an α atom is 1 (p_1). The number of Ω sites around each solute site (S_2) is $\hat{S}_\Omega$, and the probability of finding an α atom on one of these sites (p_2) is $S(\alpha_\Omega)/\hat{S}_\Omega$. The product of these four terms is

$$S_1 p_1 S_2 p_2 = (4)(1)\left(\hat{S}_\Omega\right)\left(\frac{S(\alpha_\Omega)}{\hat{S}_\Omega}\right) = 4S(\alpha_\Omega) \qquad [A2]$$

The same result is obtained for the number of α–α contacts that originate from an α atom on an Ω site to an α atom on a solute site ($S_3 p_3 S_4 p_4$). To determine the third product, there are $\hat{S}_\Omega$ Ω sites per α site (S_5), and the probability of an α atom on one of these sites (p_5) is $S(\alpha_\Omega)/\hat{S}_\Omega$. To estimate the number of Ω sites that contact each Ω site, we note that on average four solute sites contact each Ω site, and these sites are all occupied by α atoms in solute-rich glasses. The total number of α atoms that can pack around an Ω atom is given by $\hat{S}_\Omega$ evaluated at $\tilde{r}_\Omega/r_\alpha = 1/\tilde{R}$, which is denoted as $\hat{S}_\Omega^{1/R}$. The fraction of space in the first shell of each Ω atom occupied by these four solutes is $4/\hat{S}_\Omega^{1/R}$, and the fractional space remaining for Ω atoms is $1 - 4/\hat{S}_\Omega^{1/R}$. The total number of Ω atoms that can coordinate with a given Ω atom (S_6) is thus $\hat{S}_\Omega^{R=1}\left(1 - 4/\hat{S}_\Omega^{1/R}\right)$. The probability of an α atom on one of these sites (p_6) is $S(\alpha_\Omega)/\hat{S}_\Omega$. The product of these four terms is

Distribution Statement A. Approved for public release; distribution unlimited.

Table AI. Values of Reference Sites (S_n) and Occupation Probabilities (p_n)

	$\bar{S}_\alpha$	S_1	p_1	S_2	p_2	S_3	p_3	S_4	p_4	S_5	p_5	S_6	p_6	m
		α on α-site			α on Ω-site	α on Ω-site		α on α-site			α on Ω-site	α on Ω-site around Ω-site		# α-sites
$Z_{\alpha\alpha}$	≤4	4	$\frac{\bar{S}_\alpha}{4}$	$\hat{S}_\Omega$	0	$\hat{S}_\Omega$	0	4	$\frac{\bar{S}_\alpha}{4}$	$\hat{S}_\Omega$	0	$\hat{S}_\Omega^{R=1}\left(1-\frac{\bar{S}_\alpha}{\hat{S}_\Omega^{1/R}}\right)$	0	4
	>4	4	1	$\hat{S}_\Omega$	$\frac{S(\alpha_\Omega)}{\hat{S}_\Omega}$	$\hat{S}_\Omega$	$\frac{S(\alpha_\Omega)}{\hat{S}_\Omega}$	4	1	$\hat{S}_\Omega$	$\frac{S(\alpha_\Omega)}{\hat{S}_\Omega}$	$\hat{S}_\Omega^{R=1}\left(1-\frac{4}{\hat{S}_\Omega^{1/R}}\right)$	$\frac{S(\alpha_\Omega)}{\hat{S}_\Omega}$	$S(\alpha_\Omega)+4$
											Ω on Ω-site	Ω on Ω-site around Ω-site		# Ω-sites
$Z_{\Omega\Omega}$	≤4	—	—	—	—	—	—	—	—	$\hat{S}_\Omega$	1	$\hat{S}_\Omega^{R=1}\left(1-\frac{\bar{S}_\alpha}{\hat{S}_\Omega^{1/R}}\right)$	1	$\hat{S}_\Omega$
	>4	—	—	—	—	—	—	—	—	$\hat{S}_\Omega$	$1-\frac{S(\alpha_\Omega)}{\hat{S}_\Omega}$	$\hat{S}_\Omega^{R=1}\left(1-\frac{4}{\hat{S}_\Omega^{1/R}}\right)$	$1-\frac{S(\alpha_\Omega)}{\hat{S}_\Omega}$	$\hat{S}_\Omega - S(\alpha_\Omega)$
		α on α-site			Ω on Ω-site						α on Ω-site	Ω on Ω-site around Ω-site		# α-sites
$Z_{\alpha\Omega}$*	≤4	4	$\frac{\bar{S}_\alpha}{4}$	$\hat{S}_\Omega$	1	—	—	—	—	$\hat{S}_\Omega$	0	$\hat{S}_\Omega^{R=1}\left(1-\frac{\bar{S}_\alpha}{\hat{S}_\Omega^{1/R}}\right)$	1	$\bar{S}_\alpha$
	>4	4	1	$\hat{S}_\Omega$	$1-\frac{S(\alpha_\Omega)}{\hat{S}_\Omega}$	—	—	—	—	$\hat{S}_\Omega$	$\frac{S(\alpha_\Omega)}{\hat{S}_\Omega}$	$\hat{S}_\Omega^{R=1}\left(1-\frac{4}{\hat{S}_\Omega^{1/R}}\right)$	$1-\frac{S(\alpha_\Omega)}{\hat{S}_\Omega}$	$S(\alpha_\Omega)+4$
		α on α-site			Ω on Ω-site						Ω on Ω-site	α on Ω-site around Ω-site		# Ω-sites
$Z_{\Omega\alpha}$	≤4	4	$\frac{\bar{S}_\alpha}{4}$	$\hat{S}_\Omega$	1	—	—	—	—	$\hat{S}_\Omega$	1	$\hat{S}_\Omega^{R=1}\left(1-\frac{\bar{S}_\alpha}{\hat{S}_\Omega^{1/R}}\right)$	0	$\hat{S}_\Omega$
	>4	4	1	$\hat{S}_\Omega$	$1-\frac{S(\alpha_\Omega)}{\hat{S}_\Omega}$	—	—	—	—	$\hat{S}_\Omega$	$1-\frac{S(\alpha_\Omega)}{\hat{S}_\Omega}$	$\hat{S}_\Omega^{R=1}\left(1-\frac{4}{\hat{S}_\Omega^{1/R}}\right)$	$\frac{S(\alpha_\Omega)}{\hat{S}_\Omega}$	$\hat{S}_\Omega - S(\alpha_\Omega)$

*When $R < 1$ and $f_\alpha > f_{iso}$, all values of 4 are replaced by values of 2.

$$S_5p_5S_6p_6 = (\hat{S}_\Omega)\left(\frac{S(\alpha_\Omega)}{\hat{S}_\Omega}\right)\left[\hat{S}_\Omega^{R=1}\left(1-\frac{4}{\hat{S}_\Omega^{1/R}}\right)\right]\left(\frac{S(\alpha_\Omega)}{\hat{S}_\Omega}\right) = (S(\alpha_\Omega))^2\left(\frac{\hat{S}_\Omega^{R=1}}{\hat{S}_\Omega}\right)\left(1-\frac{4}{\hat{S}_\Omega^{1/R}}\right) \quad [A3]$$

Finally, we add the three previous products and normalize by the number of α atoms per α site in the structure to give the solute-rich α–α partial coordination number

$$Z_{\alpha\alpha}^{\bar{S}_\alpha>4} = \frac{4S(\alpha_\Omega)+4S(\alpha_\Omega)+(S(\alpha_\Omega))^2\left(\frac{\hat{S}_\Omega^{R=1}}{\hat{S}_\Omega}\right)\left(1-\frac{4}{\hat{S}_\Omega^{1/R}}\right)}{S(\alpha_\Omega)+4} \quad [A4]$$

Similar analyses result in the following complete set of expressions for other partial coordination numbers for solute-rich and solute-lean glasses that also can be shown to satisfy Eq. [1]

$$Z_{\alpha\alpha}^{\bar{S}_\alpha\le4} = 0 \quad [A5]$$

$$Z_{\Omega\Omega}^{\bar{S}_\alpha\le4} = \hat{S}_\Omega^{R=1}\left(1-\frac{\bar{S}_\alpha}{\hat{S}_\Omega^{1/R}}\right) \quad [A6]$$

$$Z_{\Omega\Omega}^{\bar{S}_\alpha>4} = \hat{S}_\Omega^{R=1}\left(1-\frac{4}{\hat{S}_\Omega^{1/R}}\right)\left(1-\frac{S(\alpha_\Omega)}{\hat{S}_\Omega}\right) \quad [A7]$$

$$Z_{\alpha\Omega}^{\bar{S}_\alpha\le4} = \hat{S}_\Omega \quad [A8]$$

$$Z_{\alpha\Omega}^{\bar{S}_\alpha>4} = \frac{\left(1-\frac{S(\alpha_\Omega)}{\hat{S}_\Omega}\right)\left\{4\hat{S}_\Omega+S(\alpha_\Omega)\left[\hat{S}_\Omega^{R=1}\left(1-\frac{4}{\hat{S}_\Omega^{1/R}}\right)\right]\right\}}{S(\alpha_\Omega)+4} \quad [A9]$$

$$Z_{\alpha\Omega}^{\bar{S}_\alpha\le4} = \bar{S}_\alpha \quad [A10]$$

$$Z_{\Omega\alpha}^{\bar{S}_\alpha>4} = 4+\hat{S}_\Omega^{R=1}\left(1-\frac{4}{\hat{S}_\Omega^{1/R}}\right)\left(\frac{S(\alpha_\Omega)}{\hat{S}_\Omega}\right) \quad [A11]$$

Equations [A8] and [A9] are linked to Eqs. [A10] and [A11] through the relation in Eq. [1]. It can be shown that $f_\alpha/f_\Omega = \bar{S}_\alpha/\hat{S}_\Omega$ for solute-lean glasses, so that Eq. [1] is satisfied for Eqs. [A8] and [A10] by inspection. A more detailed comparison shows that Eqs. [A9] and [A11] also satisfy Eq. [1].

The ERR approach uses specific α- and Ω-centered clusters that define the base alloy composition, where

Distribution Statement A. Approved for public release; distribution unlimited.

mixed occupancy in the coordinating shell is always acceptable. This methodology essentially deals with integer total and partial coordination numbers for each species around a specified central atom and can be extended easily into multicomponent alloy systems. Similar to $R = r_\alpha / r_\Omega$ where the radius of α is smaller than that of Ω, the effective radius ratio for an α-centered cluster ($\tilde{R}$) is defined by:

$$\tilde{R}_\alpha = \frac{R(Z_{\alpha\alpha} + Z_{\alpha\Omega})}{Z_{\alpha\alpha}R + Z_{\alpha\Omega}} \qquad [A12]$$

Equation [A12] must also satisfy local coordination summation where $Z_{\alpha\alpha} + Z_{\alpha\Omega} = Z_{\alpha,\mathrm{tot}}$. Here $Z_{\alpha,\mathrm{tot}}$ is an integer corresponding to the total coordination number around the α atom in an α-centered cluster. Furthermore, the partial coordination numbers $Z_{\alpha\alpha}$ and $\mathbf{Z}_{\alpha\Omega}$ can be described in terms of atom fraction of α (f_α) in an α-centered cluster by $Z_{\alpha\alpha} = |f_\alpha(Z_{\alpha,\mathrm{tot}} + 1) - 1|$ and $Z_{\alpha\Omega} = Z_{\alpha,\mathrm{tot}} - |f_\alpha(Z_{\alpha,\mathrm{tot}} + 1) - 1|$; hence

$$\tilde{R}_\alpha = \frac{R(Z_{\alpha,\mathrm{tot}})}{|f_\alpha(Z_{\alpha,\mathrm{tot}} + 1) - 1|\,|R + [Z_{\alpha,\mathrm{tot}} - |f_\alpha(Z_{\alpha,\mathrm{tot}} + 1) - 1|]} \qquad [A13]$$

Similarly, for Ω-centered clusters where the radius of α is smaller than that of Ω

$$\tilde{R}_\Omega = \frac{(Z_{\Omega\alpha} + Z_{\Omega\Omega})}{Z_{\Omega\alpha}R + Z_{\Omega\Omega}} \qquad [A14]$$

where $Z_{\Omega\alpha} + Z_{\Omega\Omega} = Z_{\Omega,\mathrm{tot}}$ and $Z_{\Omega,\mathrm{tot}}$ is an integer corresponding to the total coordination number around an Ω atom in an Ω-centered cluster. The partial coordination numbers $Z_{\Omega\alpha}$ and $Z_{\Omega\Omega}$ can be described in terms of f_α in an Ω-centered cluster by $Z_{\alpha\alpha} = |f_\alpha(Z_{\alpha,\mathrm{tot}} + 1) - 1|$ and $Z_{\Omega\Omega} = Z_{\Omega,\mathrm{tot}} - f_\alpha(Z_{\Omega,\mathrm{tot}} + 1)$; hence

$$\tilde{R}_\Omega = \frac{(Z_{\alpha,\mathrm{tot}})}{[f_\alpha(Z_{\alpha,\mathrm{tot}} + 1)]R + [Z_{\Omega,\mathrm{tot}} - f_\alpha(Z_{\Omega,\mathrm{tot}} + 1)]} \qquad [A15]$$

Rarely will $\tilde{R}$ be equal to the ideal radius ratio for perfect packing for a given coordination number, so to normalize coordination numbers to perfect packing, $\tilde{R}$ is equated to the R^* value for a specific a total coordination number, whereby a specific atomic fraction of α can be calculated for each total coordination number (integer) for a given radius ratio R. That is,

$$f_\alpha = \frac{R\left(\frac{Z_{\alpha,\mathrm{tot}}}{R^*} + 1\right) - (Z_{\alpha,\mathrm{tot}} + 1)}{(R - 1)(Z_{\alpha,\mathrm{tot}} + 1)} \qquad [A16]$$

and

$$f_\alpha = \frac{Z_{\Omega,\mathrm{tot}}\left(\frac{1}{R^*} - 1\right)}{(R - 1)(Z_{\Omega,\mathrm{tot}})} \qquad [A17]$$

where by mathematical limits, if $R < 1$, then $0 < Z_{\alpha,\mathrm{tot}} \leq 13$ and $14 < Z_{\alpha,\mathrm{tot}} \leq 20$. It is assumed that the total and partial coordination numbers of each species $Z_{\alpha,\mathrm{tot}}$, $Z_{\Omega,\mathrm{tot}}$, $Z_{\alpha\alpha}$, $Z_{\alpha\Omega}$, $Z_{\Omega\alpha}$, and $Z_{\Omega\Omega}$ adjust linearly as a function of f_α between integer values of $Z_{\alpha,\mathrm{tot}}$ and $Z_{\Omega,\mathrm{tot}}$. So it is, through $Z_{\alpha,\mathrm{tot}}$ and $Z_{\Omega,\mathrm{tot}}$, thus possible to estimate total and partial coordination numbers as a function of f_α for a given radius ratio R, which is shown in Figure 3 for R values of 0.902, 0.799, and 0.7099.

To estimate the sizes of β sites (interstices at the center of an octahedron of structure-forming clusters) and γ sites (interstices at the center of a tetrahedron of structure-forming clusters), we start by approximating the cluster radius as one half the cluster–cluster separation. The minimum cluster–cluster separation represents the most efficient packing and occurs when the faces of adjacent clusters are in contact. Face contact may not be possible for all cluster contacts, and so an intermediate separation for edge contact of adjacent clusters is also considered. The equations for these cluster–cluster separations are taken from Eqs. [A3(a)] and [A3(d)] in Reference 7 and after normalization by r_Ω are

$$R_{\mathrm{cluster}}^{\mathrm{face}} = \sqrt{(1 + R_\alpha)^2 - \frac{4}{3}} + \sqrt{\frac{2}{3}} \qquad [A18]$$

$$R_{\mathrm{cluster}}^{\mathrm{edge}} = \sqrt{(1 + R_\alpha)^2 - 1} + \sqrt{\frac{1}{2}} \qquad [A19]$$

The distance from the center of a β site to the center of an α site of one of the bounding clusters (Figure 4(b)) is simply $\sqrt{2}R_{\mathrm{cluster}}$. This same distance is also given by the distance between an α and β atom separated by a trigonal ring of Ω atoms (a trigonal bipyramid) for face contact, and for the distance between an α and β atom separated by a pair of contacting Ω atoms for edge contact. These latter two relations are taken from Eqs. [A1(a)] and [A1(d)] in Reference 7.

$$d_{\alpha\beta}^{\mathrm{face}} = \sqrt{(1 + R_\alpha)^2 - \frac{4}{3}} + \sqrt{(1 + R_\beta)^2 - \frac{4}{3}} \qquad [A20]$$

$$d_{\alpha\beta}^{\mathrm{edge}} = \sqrt{(1 + R_\alpha)^2 - 1} + \sqrt{(1 + R_\beta)^2 - 1} \qquad [A21]$$

Setting these equations equal to $\sqrt{2R_{\mathrm{cluster}}}$ and solving for R_β gives

$$R_\beta^{\mathrm{face}} = \sqrt{\left[\left(\sqrt{2} - 1\right)\sqrt{(1 + R_\alpha)^2 - \frac{4}{3}} + \sqrt{\frac{4}{3}}\right]^2 + \frac{4}{3}} - 1 \qquad [A22]$$

$$R_\beta^{\mathrm{edge}} = \sqrt{\left[\left(\sqrt{2} - 1\right)\sqrt{(1 + R_\alpha)^2 - 1} + 1\right]^2 + 1} - 1 \qquad [A23]$$

Distribution Statement A. Approved for public release; distribution unlimited.

A similar approach is used to estimate the size of atoms that can occupy γ sites. In this case, where a γ site is surrounded by a tetrahedron of solute-centered clusters, the distance from the center of a γ site to the center of an α site of one of the bounding clusters is $\sqrt{\frac{3}{2}}R_{\text{cluster}}$. The development is otherwise the same as for β sites, and the final equations are

$$R_{\gamma}^{\text{face}} = \sqrt{\left[\left(\sqrt{\frac{3}{2}} - 1\right)\sqrt{(1 + R_{\alpha})^2 - \frac{4}{3}} + 1\right]^2 + \frac{4}{3}} - 1 \quad [A24]$$

$$R_{\gamma}^{\text{edge}} = \sqrt{\left[\left(\sqrt{\frac{3}{2}} - 1\right)\sqrt{(1 + R_{\alpha})^2 - 1} + \frac{\sqrt{3}}{2}\right]^2 + 1} - 1 \quad [A25]$$

Equations [A22] and [A23] are plotted in Figure 4(a) as the upper and lower bounds for the size of atoms that can be placed at β sites without pushing apart the bounding clusters, and Eqs. [A24] and [A25] show the size of γ sites.

REFERENCES

1. K.J. Laws, K.F. Shamlaye, K. Wong, B. Gun, and M. Ferry: *Metall. Mater. Trans. A*, 2010, vol. 41A, pp. 1699–1705.
2. D.B. Miracle: *J. Non-Cryst. Sol.*, 2004, vol. 242, pp. 89–96.
3. P. Lamparter and S. Steeb: *Structure of Solids*, ed., V. Gerold, vol. 1, *Materials Science and Technology, A Comprehensive Treatment*, R.W. Cahn, P. Haasen, and E.J. Kramer, eds., VCH, Weinheim, Germany, 1993, pp. 217–88.
4. O.N. Senkov, D.B. Miracle, E.R. Barney, A.C. Hannon, Y.Q. Cheng, and E. Ma: *Phys. Rev. B*, 2010, vol. 82, pp. 104206-1–104206-13.
5. D. Ma, A.D. Stoica, L. Yang, W.-L. Wang, Z.P. Lu, J. Neuefeind, M.J. Kramer, J.W. Richardson, and T. Proffen: *Appl. Phys. Lett.*, 2007, vol. 90, pp. 211908-1–211908-3.
6. D.B. Miracle: *Nat. Mater.*, 2004, vol. 3, pp. 697–702.
7. D.B. Miracle: *Acta Mater.*, 2006, vol. 54, pp. 4317–36.
8. D.B. Miracle, D. Louzguine-Luzgin, L. Louzguina-Luzgina, and A. Inoue: *Int. Mater. Rev.*, 2010, vol. 55, pp. 218–56.
9. G. Duan, D. Xu, Q. Zhang, G. Zhang, T. Cagin, W.L. Johnson, and I.W.A. Goddard: *Phys. Rev. B*, 2005, vol. 71, pp. 224208-1–224208-9.
10. N. Mattern, P. Jovari, I. Kaban, S. Gruner, A. Elsner, V. Kokotin, H. Franz, B. Beuneu, and J. Eckert: *J. Alloy Compd.*, 2009, vol. 485, pp. 163–69.
11 M.I. Mendelev, D.J. Sordelet, and M.J. Kramer: *J. Appl. Phys.*, 2007, vol. 102, pp. 043501-1–043501-7.
12. E.A. Lass, A. Zhu, G.J. Shiflet, and S.J. Poon: *Acta Mater.*, 2010, vol. 58, pp. 5460–70.
13. D.B. Miracle, W.S. Sanders, and O.N. Senkov: *Phil. Mag. A*, 2003, vol. 83, pp. 2409–28.
14. Q. Wang, J.B. Qiang, J.H. Xia, J. Wu, Y.M. Wang, and C. Dong: *Intermetallics*, 2007, vol. 15, pp. 711–15.
15. H.W. Sheng, W.K. Luo, F.M. Alamgir, J.M. Bai, and E. Ma: *Nature*, 2006, vol. 439, pp. 419–25.
16. T. Egami, V.A. Levashov, J.R. Morris, and O. Haruyama: *Metall. Mater. Trans. A*, 2010, vol. 41A, pp. 1628–33.
17. R. Ray, R. Hasegawa, C.-P. Chou, and L.A. Davis: *Scripta Metall.*, 1977, vol. 11, pp. 973–78.
18. E. Matsubara, Y. Waseda, A. Inoue, H. Ohtera, and T. Masumoto: *Z. Naturforsch*, 1989, vol. 44a, pp. 814–20.

Distribution Statement A. Approved for public release; distribution unlimited.